

# Iridium-catalysed enantioselective formal deoxygenation of racemic alcohols via asymmetric hydrogenation

Jia Zheng<sup>1</sup>, Jira Jongcharoenkamol<sup>1,4</sup>, Bram B. C. Peters<sup>1</sup>, Jasper Guhl<sup>1</sup>, Sudipta Ponra<sup>1</sup>, Mårten S. G. Ahlquist<sup>2</sup> and Pher G. Andersson<sup>1,3\*</sup>

**Asymmetric hydrogenation of alkenes is one of the most powerful tools for the preparation of optically active compounds. However, to achieve high enantioselectivity, the starting olefin in most cases needs to be isomerically pure in either the *cis* or the *trans* form. Generally, most olefination protocols provide olefins as isomeric mixtures that are difficult to separate, and in many cases also generate lots of waste. In contrast, the synthesis of racemic alcohols is straightforward and highly atom-efficient, with products that are easier to purify. Here, we describe a strategy that enables rapid access to chiral alkanes via enantioconvergent formal deoxygenation of racemic alcohols. Mechanistic studies indicate an Ir-mediated elimination of water and subsequent *in situ* hydrogenation. This approach allows rapid and efficient assembly of chiral intermediates and is exemplified in the total synthesis of antidepressant sertraline and  $\sigma_2$  receptor PB 28.**

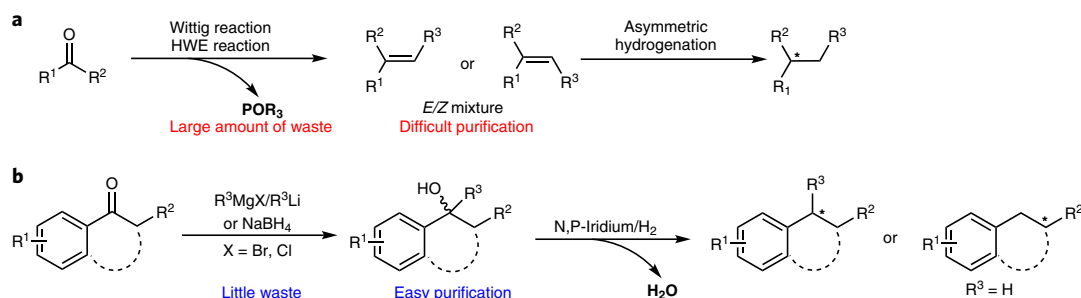
Asymmetric hydrogenation of olefins has emerged as one of the most efficient and atom-economic strategies to install steric centres to prochiral compounds, particularly in industry<sup>1–7</sup>. In general terms, geometrically pure alkenes are required to produce products in high enantiomeric excess due to the enantiodivergence phenomenon<sup>8–13</sup>. The synthesis of olefins normally produces isomeric olefin mixtures that require difficult chromatographic separation. In addition, classic olefination processes also generate a considerable amount of by-products, such as phosphine oxide or phosphinate and residues from leaving groups and bases (Fig. 1a)<sup>14–16</sup>. In contrast, tertiary alcohols can be simply prepared by addition to ketones with very little by-product formation and are easily purified. The combination of the alcohol preparation and deoxygenation process could transform ketones into chiral alkanes, with water as the only by-product, providing an efficient and atom-economic approach. Therefore, asymmetric deoxygenation of racemic alcohols could be an ideal alternative to produce chiral alkanes. Over the past few decades, inspired by the Barton–McCombie reaction, numerous methods for deoxygenation have been developed by using transition metal, Lewis- or Brønsted acid catalysts<sup>17–19</sup>. Recently, strategies such as mono-deoxygenation of diols<sup>20–24</sup>, sequential dehydrogenation/Wolff–Kishner reduction<sup>25–27</sup> and directing group-assisted site-selective deoxygenation<sup>28</sup> have been utilized to tackle the regioselective deoxygenation process. However, the construction of enantioenriched tertiary carbons via deoxygenation of racemic alcohols remains challenging. The only related strategy recently reported by Carreira's group was the transition-metal catalysed allenyl substitution, using an allene group for the coordination-induced enantiocontrol<sup>29</sup>. Despite the above advance in this concept, the development of enantioselective deoxygenation of unfunctionalized alcohols is still challenging and in great demand.

We herein report a strategy for enantioselective deoxygenation of racemic alcohols via N,P-iridium catalysis, which allows the facile construction of chiral alkanes with good to excellent levels of enantiomeric excess (e.e.) (Fig. 1b). This protocol opens up a direct route to create stereogenic centres via a highly efficient and atom-economic approach.

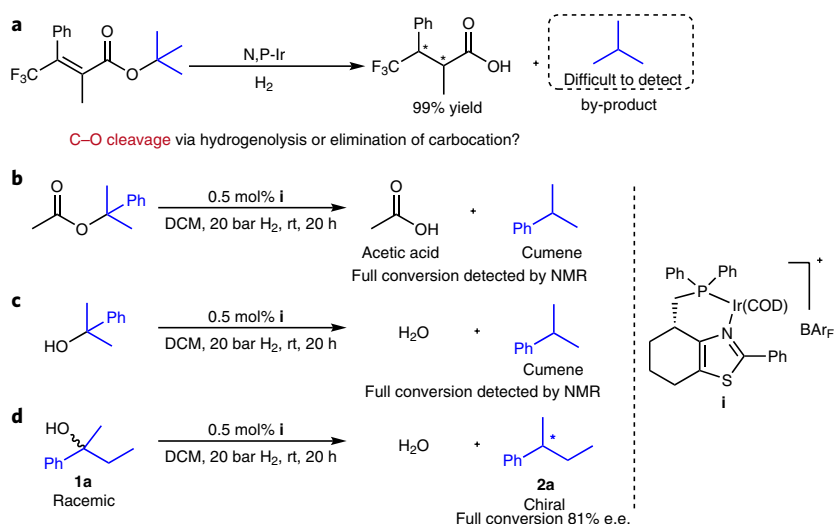
## Results

**Initial studies.** In our previous studies, the acidic Ir(v)-hydride species showed the ability to cleave alcoholic C–O bonds<sup>30,31</sup>. Recently, we accidentally observed that the  $\alpha,\beta$ -unsaturated *t*-butyl ester was quantitatively converted into the chiral carboxylic acid on attempted asymmetric hydrogenation (Fig. 2a)<sup>32</sup>. Although it was not isolated, we suspected that isobutane was formed as a by-product through either hydrogenolysis or elimination followed by hydrogenation. To confirm this hypothesis, the *t*-butyl group was replaced by a dimethylbenzyl group. Subjecting 2-phenylpropan-2-acetate to typical hydrogenation conditions using the N,P-iridium catalyst **i** resulted in the formation of cumene, which was confirmed via <sup>1</sup>H-NMR (Fig. 2b). Furthermore, the corresponding alcohol, 2-phenylpropan-2-ol, was fully converted into cumene under the same reaction conditions (Fig. 2c). Inspired by the above results, racemic substrate **1a** was selected to investigate the possibility of an asymmetric deoxygenation in our catalytic system. Gratifyingly, N,P-iridium catalyst **i** gave full conversion of racemic alcohol **1a** to **2a** with 81% e.e. in dichloromethane (DCM) under 20 bar of H<sub>2</sub> (Fig. 2d). We also found that a number of related catalysts such as [Ir(Py)(PCy<sub>3</sub>)]BAR<sub>F</sub>, Crabtree's catalyst and Wilkinson's catalyst did not trigger the deoxygenation under the same conditions. Moreover, when the Ir(COD)Cl dimer was used as catalyst without any ligand, no deoxygenation took place and only Ir-based nanoparticles were observed to form.

<sup>1</sup>Department of Organic Chemistry, Stockholm University, Stockholm, Sweden. <sup>2</sup>Department of Theoretical Chemistry & Biology, School of Engineering Sciences in Chemistry Biotechnology and Health, KTH Royal Institute of Technology, Stockholm, Sweden. <sup>3</sup>School of Chemistry and Physics, University of Kwazulu-Natal, Durban, South Africa. <sup>4</sup>Present address: Program in Chemical Biology, Chulabhorn Graduate Institute, Chulabhorn Royal Academy, Bangkok, Thailand. \*e-mail: [Pher.Andersson@su.se](mailto:Pher.Andersson@su.se)



**Fig. 1 | Different preparative routes from ketones to chiral alkanes. a**, Classic olefination followed by asymmetric hydrogenation. **b**, This work: alcohol preparation followed by enantioselective deoxygenation.

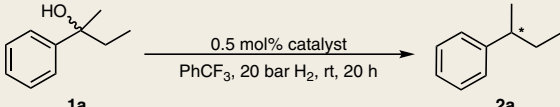


**Fig. 2 | Initial studies of Ir-catalysed deoxygenation. a**, Observed C–O bond cleavage in a previous study. **b**, Initial attempt at acetate deoxygenation. **c**, Initial attempt at alcohol deoxygenation. **d**, Initial attempt at asymmetric deoxygenation. DCM, dichloromethane; rt, room temperature.

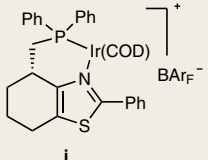
**Optimization studies.** Next, an optimization was carried out by using **1a** as the model substrate. In the solvent screening,  $PhCF_3$  gave 85% e.e., which is higher than that obtained in DCM, benzene and toluene (Table 1, entries 1–4). The reaction also proceeded smoothly in EtOAc but gave low enantioselectivity (48% e.e., Table 1, entry 5). As expected, solvents such as tetrahydrofuran and *i*-PrOH inhibited the transformation since the coordination between the substrate and catalyst was blocked (Table 1, entries 6–7). Therefore, the following catalyst screening was run in  $PhCF_3$ . Catalysts with different backbones were selected (catalysts **i–v**) from our catalyst library for the initial catalyst optimization. It is worth noting that the selected catalysts had shown excellent enantioselectivity in the hydrogenation of the unfunctionalized trisubstituted *E*-olefin (the probable intermediate), as we speculated an olefination process was involved in this deoxygenation. To our surprise, these catalysts afforded different levels of e.e. in the model reaction, which indicated that the elimination might generate isomeric olefin mixtures instead of pure *E*-olefin. To our delight, we found that linear alcohol **1a** fitted well to the imidazole catalyst **ii**, giving high enantioselectivity (91% e.e., Table 1, entry 8). Oxazole and oxazoline catalysts **iii** and **iv** afforded only moderate levels of e.e., while thiazole catalyst **v** resulted in 81% e.e. (Table 1, entries 9–11). To further improve the enantiomeric outcomes, several other catalysts were evaluated (Supplementary Table 1). Unfortunately, varying the nature of the phosphine or heterocyclic moieties did not improve the e.e. Therefore, imidazole

catalyst **ii** in  $PhCF_3$  was found to be the best combination for the enantioselective deoxygenation of linear alcohols.

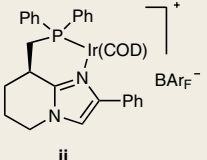
**Scope of enantioselective deoxygenation.** Having optimized the conditions, we investigated the substrate scope of linear tertiary alcohols. As shown in Fig. 3, an electron-withdrawing group led to lower reactivity, and required 1 mol% catalyst loading to reach full conversion to yield **2b** with 88% e.e. Substrates with electron-donating groups on the *para*- and *meta*-position (**1c–1e**) gave excellent isolated yields (88–95%) and enantioselectivities (87–91% e.e.). The 1,1'-biphenyl and 2-naphthyl substrates were deoxygenated to generate **2f** and **2g** with 94% e.e., whereas the yield of **2g** was slightly lower. Different alkyl chains slightly influenced the enantioselectivity of this transformation, with similar reactivity (92–98% yields). By increasing the steric hindrance, the enantiomeric excess values varied from 83% to 87% when the side chain was substituted by benzyl, *n*-propyl and *i*-propyl groups (**2h–j**). With benzyl groups adjacent to the quaternary carbon, compounds **1k** and **1l** provided 93% and 96% yields with 86% and 88% e.e., respectively. When the phenyl adjacent to the deoxygenated centre was replaced by *t*-butyl (**1m**), only a complicated mixture was obtained. Interestingly, the bidentate diol, compound **1n**, gave no conversion under the standard conditions, which may be due to chelation between Ir and the hydroxyl groups resulting in a deactivation of the catalyst.

**Table 1 | Selected optimization for linear alcohols**


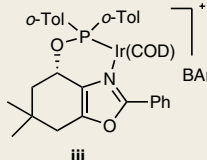
**1a**  $\xrightarrow[\text{PhCF}_3, 20 \text{ bar H}_2, \text{rt, 20 h}]{0.5 \text{ mol\% catalyst}}$  **2a**



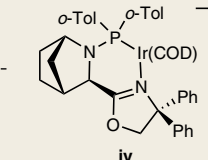
**i**



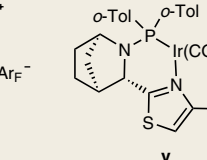
**ii**



**iii**



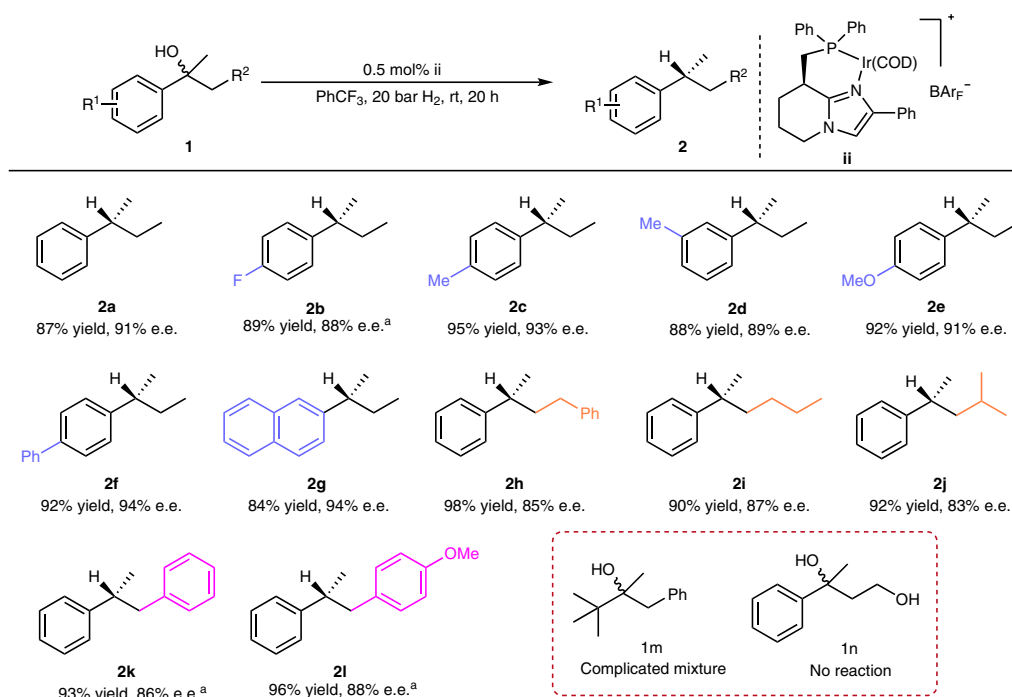
**iv**



**v**

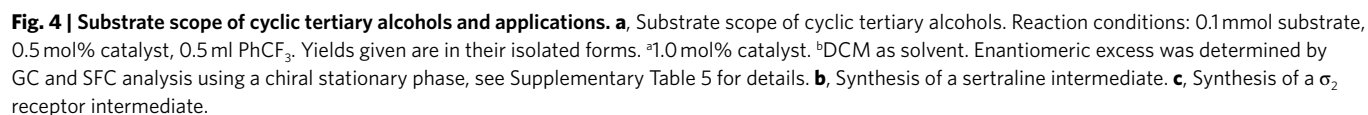
Entry	Solvent	Catalyst	Conversion (%)	e.e. (%)
1	DCM	<b>i</b>	100	81
2	Benzene	<b>i</b>	100	81
3	Toluene	<b>i</b>	100	84
4	PhCF <sub>3</sub>	<b>i</b>	100	85
5	EtOAc	<b>i</b>	100	48
6	THF	<b>i</b>	0	–
7	<i>i</i> -PrOH	<b>i</b>	0	–
8	PhCF <sub>3</sub>	<b>ii</b>	100	91
9	PhCF <sub>3</sub>	<b>iii</b>	100	55
10	PhCF <sub>3</sub>	<b>iv</b>	100	65
11	PhCF <sub>3</sub>	<b>v</b>	100	81

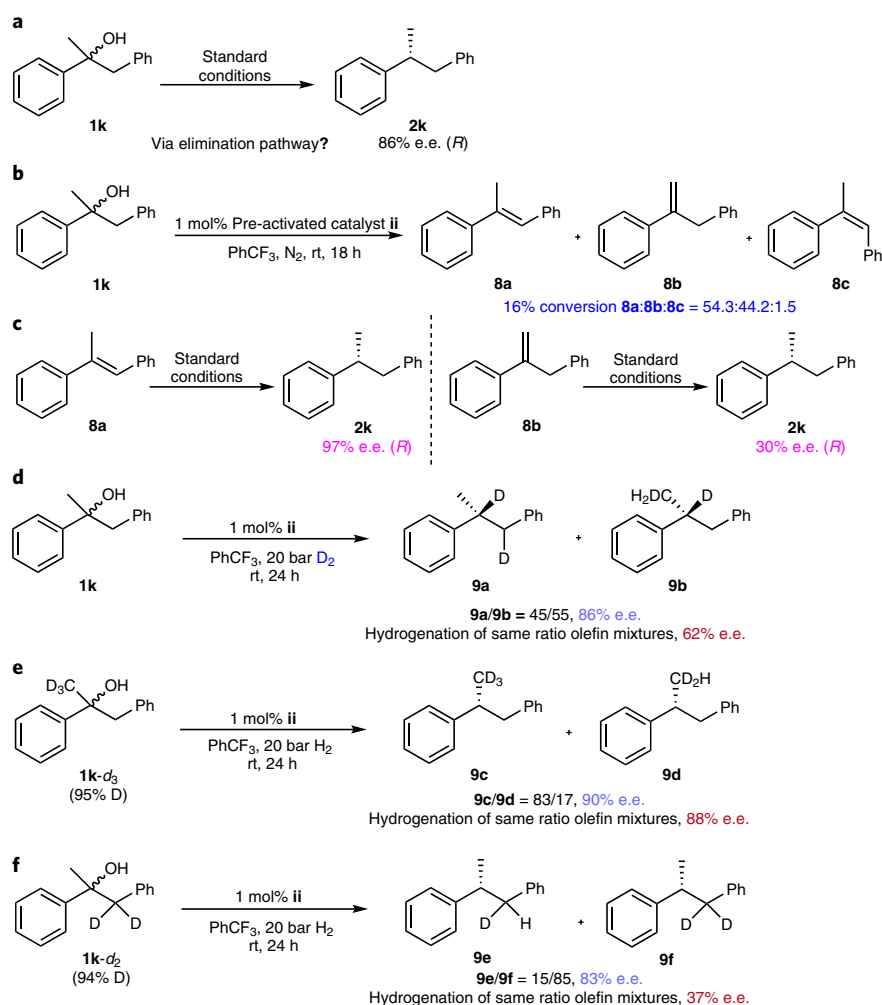
Reaction conditions: 0.1 mmol substrate, 0.5 mol% catalyst, 0.5 ml PhCF<sub>3</sub>. Conversions were determined by <sup>1</sup>H-NMR spectroscopy. Enantiomeric excess was determined by GC analysis using a chiral stationary phase.

**Fig. 3 | Substrate scope of linear tertiary alcohols.** Reaction conditions: 0.1 mmol substrate, 0.5 mol% catalyst, 0.5 ml PhCF<sub>3</sub>. Yields are given in their isolated forms. <sup>a</sup>1.0 mol% catalyst. The e.e. was determined by GC and SFC analysis using a chiral stationary phase, see Supplementary Table 5 for details.

We then investigated the enantioselective deoxygenation of cyclic tertiary alcohols (Fig. 4a). A catalyst screening (Supplementary Table 2) was required since catalyst **ii** was observed to be less

efficient for this class of substrates. Catalysts **iii** and **iv** turned out to be the best in terms of the selectivity. In addition, similar e.e. values were obtained when hydrogenating cyclic tertiary substrates with



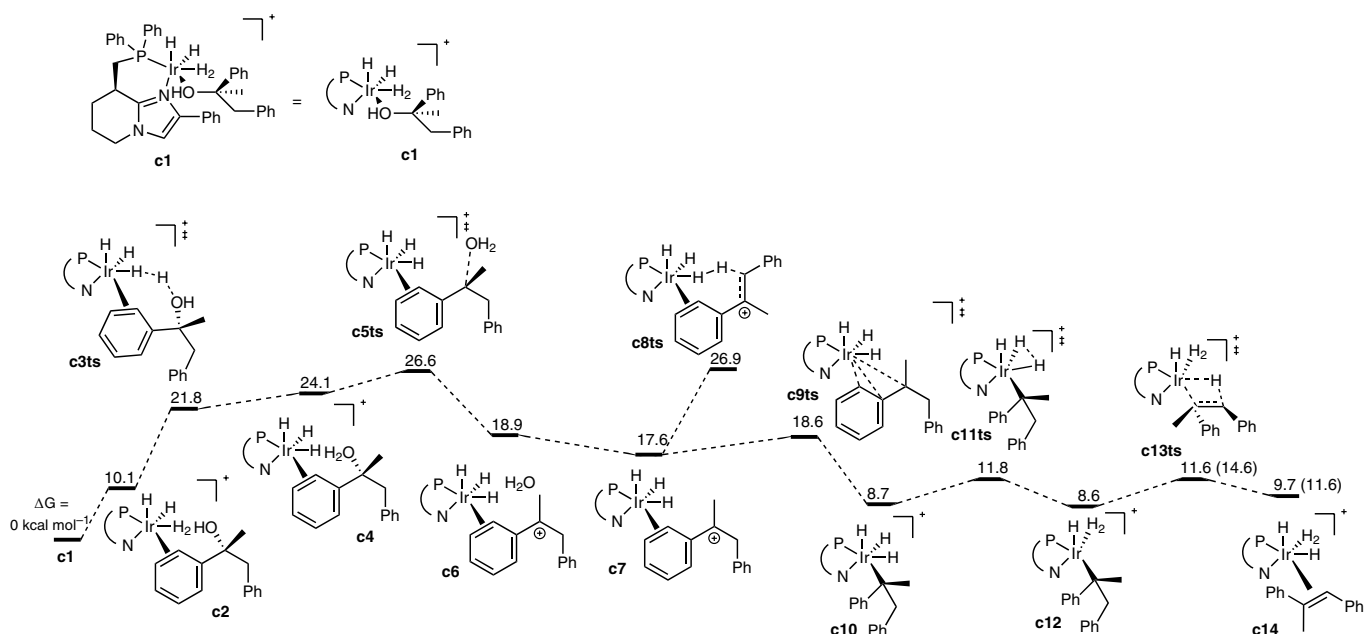


**Fig. 5 | Mechanistic studies.** **a**, Enantioselective deoxygenation of **1k** under standard conditions. **b**, Alcohol elimination by pre-activated catalyst. **c**, Asymmetric hydrogenations of geometrically pure alkenes. **d**, Enantioselective deoxygenation of **1k** under  $D_2$  gas. **e**, Enantioselective deoxygenation of deuterated substrate **1k- $d_3$** . **f**, Enantioselective deoxygenation of deuterated substrate **1k- $d_2$** .

both catalysts **iii** and **iv** (Supplementary Table 3). Increasing the aliphatic chain length from methyl to *n*-butyl resulted in no obvious influence, producing **4a–4d** in high yields with 91% to 93% e.e. A 98% e.e. was observed when a bulkier *i*-butyl group was installed onto the alcohol carbon (**4e**). In addition, a substrate bearing an alkyl trifluoromethyl group was converted smoothly into the desired product with 94% e.e. (**4f**). A benzyl substituted alcohol was converted smoothly into **4g** in 92% yield with 90% e.e., while the phenyl substituted molecule **4h** was obtained with 99% e.e. The removal of the *para*-methoxyl group on the aromatic ring led to a slight drop in enantioselectivity (**4i**). Substrates with seven- and five-membered rings were examined, affording **4j** and **4k** in high yields with 94% and 98% e.e., respectively. Next, the less reactive secondary alcohols were evaluated by using catalyst **iv** (See Supplementary Table 4 for the catalysts screening), which provided the enantioenriched carbon adjacent to the deoxygenated centre. Diastereomeric alcohol mixtures with methyl and benzyl groups proceeded smoothly to afford **6a** and **6b** in high yields with excellent e.e. The use of a substrate with a methoxy group on the phenyl ring generated **6c** in a 97% yield with 99% e.e. Switching the methyl side-chain to the bulkier *i*-butyl group did not influence on the reactivity or enantioselectivity. The scalability of this Ir-catalysed asymmetric deoxygenation reaction was confirmed by employing 0.88 g (4.0 mmol) of starting material **3c**. The desired product **4c** was obtained in 94% isolated

yield and 93% e.e. Both yield and enantioselectivity were retained when compared with small scale transformation. To demonstrate the synthetic utility, this strategy was applied to synthesize intermediates of bioactive compounds. Chiral tetrahydronaphthalene **4l** was obtained via the enantioselective deoxygenation in 96% yield and 98% e.e., which was a reported intermediate in the synthesis of the antidepressant sertraline (Fig. 4b)<sup>33</sup>. Moreover, racemic alcohol **3m** was fully reduced to afford **4m** in 94% yield and 88% e.e. The following deprotection of the benzyl group led to a chiral alcohol **7** with 88% e.e., which can be converted into a  $\sigma_2$  receptor ligand **PB 28** (Fig. 4c)<sup>34</sup>.

**Mechanistic studies.** As mentioned above, alcohol **1k** provided chiral alkane **2k** with 86% e.e., and this substrate was chosen for further studies on the mechanism of the reaction (Fig. 5a). To understand how the catalysts influenced elimination of the hydroxyl group, **1k** was employed with the pre-activated catalyst under  $N_2$  atmosphere, which led to an isomeric mixture of olefins in 16% conversion (Fig. 5b). The ratio between *E*-olefin **8a**, terminal olefin **8b** and *Z*-olefin **8c** was 54.3:44.2:1.5 (Supplementary Fig. 1), which suggests that the deoxygenation went through the hydrogenation of the olefin mixture. However, hydrogenation of such a mixture should result in a much lower e.e., as terminal olefins generally give low enantioselectivity<sup>3</sup>. To confirm this, olefins **8a** and **8b** were evaluated using



**Fig. 6 | Computational studies of c1–c6.** Protonation of the alcohol by the  $H_2$  ligand of the iridium complex, followed by C–O bond cleavage. **c7–c14**, Mechanism for formation of an olefin complex. All numbers are Gibbs free energies ( $\text{kcal mol}^{-1}$ ). Numbers in parentheses are for elimination of the terminal hydride at the methyl group.

catalyst **ii** and were found to give 97% and 30% e.e., respectively (Fig. 5c). Subsequently, several labelling experiments were conducted. First, the reaction was run using deuterium gas. In this case, two deuterated products, **9a** and **9b**, were identified. Product **9a** was obtained by hydrogenation of the internal olefin (mainly *E*-olefin), and **9b** was produced from the terminal olefin, which gave an approximately 45:55 ratio (Fig. 5d, Supplementary Fig. 2). The ratio of the olefin formation could be controlled by deuterated substrates and the elimination showed a kinetic isotope effect that was found to prefer removal of the hydrogen over removal of the deuterium. Using **1k-d<sub>3</sub>**, this effect led to increased internal olefin formation (internal:terminal ratio was 83:17, respectively, see Fig. 5e, Supplementary Fig. 3). For substrate **1k-d<sub>2</sub>**, the benzylic position was deuterated and resulted in increased formation of the terminal olefin (internal:terminal ratio was 15:85, respectively, see Fig. 5f, Supplementary Fig. 4). Surprisingly, when different olefin mixtures were formed as intermediates in the application of the methodology to substrates **1k-d<sub>2</sub>**, **1k** and **1k-d<sub>3</sub>**, the enantiomeric purity of the product **2k** varied only slightly (83%, 86% and 90% e.e.) (Fig. 5d–f). For comparison, olefin mixtures with the same ratios were evaluated in the hydrogenations. As expected, the enantiomeric purity of the product dropped considerably (from 88% to 37% e.e.), as the amount of terminal olefin in the mixtures increased from 17% to 83% (Fig. 5d–f). The above results suggest that the enantioselectivity is not primarily dependent on the ratio of the isomeric mixture in the olefination pathway, but rather is mainly reliant on the interaction between the chiral Ir catalyst that, during the elimination process, may provide olefin complexes in which predominantly one of the enantiometric faces are associated with the Ir-centre.

**Computational studies.** A reaction pathway involving protonation of the alcohol at the Ir catalyst was identified by density functional theory using the B3LYP-D3 functional with implicit solvation corrections (Fig. 6, See Supplementary Methods for details of the computations). The initial structure was complex **A**, where  $H_2$  has been added oxidatively and one  $H_2$  coordinates in a *trans* fashion to the phosphorous, while the alcohol coordinates to the metal via

the hydroxyl oxygen *trans* to one of the hydrides. The structure is similar to the proposed structures for olefin hydrogenation<sup>35</sup>, but with the current systems olefins are only intermediates and present in low concentrations. After rearrangement to coordinate via one of the phenyl groups, the hydroxyl group can accept a proton from the coordinated  $H_2$ . A transition state was identified for the process at  $\Delta G = 21.8 \text{ kcal mol}^{-1}$ , compared with **c1**, where  $\Delta G$  is the relative Gibbs free energy. The product complex was found to be more stable on the potential energy surface, but after thermochemical corrections, the Gibbs free energy was actually slightly higher than the preceding transition state. This is an artefact that mainly originates from the separation of nuclear and electronic degrees of freedom, with a posteriori correction for nuclear vibrational zero-point energy. On the potential energy surface **c3ts** is higher in energy than **c4**. After the oxonium complex **c4** is formed, the C–O bond is broken via **c5ts**, which was found to be the highest free-energy structure at  $\Delta G = 26.6 \text{ kcal mol}^{-1}$  — which agrees well with the experimental observation of a slow, but observable, reaction. Once the C–O bond is broken the carbocation initially coordinates via one of the double bonds of the phenyl ring (**c6** and **c7**). Then, **c7** can rearrange to an Ir(v) complex **c10** where the benzylic carbon forms a bond to Ir. We note that there is some interaction with the *ipso* carbon of the phenyl ring. An alternative path is direct proton transfer from the carbocation to the hydride *trans* to phosphorous (**c8ts**), but the activation energy is high compared to that of the rearrangement. **c10** is at  $8.7 \text{ kcal mol}^{-1}$  compared with **c1**, and from here the olefin can be formed via  $\beta$ -hydride elimination. Before the  $\beta$ -hydride elimination step (**c13ts**), two hydrides form a  $H_2$  ligand via reductive elimination (**c11ts**), which opens up a free coordination site at the metal. Finally, an olefin complex is formed (**c14**), and the process is associated with very low activation free energies, indicating that once the Ir(v) complex **c10** is formed, the formation of the olefin is rapid. We have previously shown that the most likely olefin precursor for olefin hydrogenation is a complex where the olefin coordinates *trans* to the phosphine. We have therefore identified a mechanism by which the olefin complex can indeed rearrange via  $H_2$  dissociation and reassociation to the more stable



complex (Supplementary Fig. 5). All activation energies towards the most stable complex **c26** are low, with the highest point at 13.9 kcal mol<sup>-1</sup>.

## Conclusions

We have conceived and developed an N,P-iridium catalysed enantioselective deoxygenation of racemic alcohols to produce chiral alkanes. The Ir-hydride intermediates played indispensable roles in alcohol activation, as well as elimination and in situ asymmetric hydrogenation, which lead to the formation of an enantioenriched tertiary carbon in the deoxygenation pathway. A variety of tertiary acyclic and cyclic alcohols and secondary cyclic alcohols have been successfully evaluated under mild conditions, giving high yields with good enantiocontrol (up to 99% e.e.). In contrast to olefins, the synthesis of alcohols does not require extensive purification and minimizes the formation of by-products. A collection of control experiments and calculations revealed that the geometry of olefin formation is not significant for high enantioselectivity, but instead suggests that the enantioselectivity originates from the Ir catalysed elimination. The presented catalytic transformation expands the possibilities of simplifying the catalytic asymmetric hydrogenation protocol and revealing an iridium mechanism in the elimination of benzylic alcohols.

## Methods

**General procedure for the deoxygenation of alcohols.** A vial was charged with an alcohol (0.1 mmol) and the Ir-N,P-catalyst (0.5 or 1.0 mol%). PhCF<sub>3</sub> (0.5 ml) was added and the vial was placed in a high-pressure hydrogenation apparatus. The reactor was purged three times with Ar, and then filled with H<sub>2</sub>. The reaction was stirred at room temperature for 20 hours before the H<sub>2</sub> pressure was released and the solvent removed under reduced pressure. The residue was purified by flash chromatography on silica gel to give the alkane. The e.e. value was determined by GC- or SFC analysis on chiral stationary phase. The corresponding racemic product was used for comparison and was prepared on a 0.1 mmol scale using Pd/C (or racemic Ir) as the catalyst, following the same asymmetric hydrogenation procedure. See the Supplementary Methods for the characterization data, NMR spectra, GC and SFC.

## Data availability

All data is available from the authors on reasonable request.

Received: 14 July 2019; Accepted: 26 September 2019;

Published online: 4 November 2019

## References

- Roseblade, S. J. & Pfaltz, A. Iridium-catalyzed asymmetric hydrogenation of olefins. *Acc. Chem. Res.* **40**, 1402–1411 (2007).
- Chirik, P. J. Iron- and cobalt-catalyzed alkene hydrogenation: catalysis with both redox-active and strong field ligands. *Acc. Chem. Res.* **48**, 1687–1695 (2015).
- Veredel, J. J., Pàmies, O., Diéguez, M. & Andersson, P. G. Asymmetric hydrogenation of olefins using chiral crabtree-type catalysts: scope and limitations. *Chem. Rev.* **114**, 2130–2169 (2014).
- Zhu, S.-F. & Zhou, Q.-L. Iridium-catalyzed asymmetric hydrogenation of unsaturated carboxylic acids. *Acc. Chem. Res.* **50**, 988–1001 (2017).
- Minnaard, A. J., Feringa, B. L., Lefort, L. & de Vries, J. G. Asymmetric hydrogenation using monodentate phosphoramidite ligands. *Acc. Chem. Res.* **40**, 1267–1277 (2007).
- Zhang, W., Chi, Y. & Zhang, X. Developing chiral ligands for asymmetric hydrogenation. *Acc. Chem. Res.* **40**, 1278–1290 (2007).
- Etayo, P. & Vidal-Ferran, A. Rhodium-catalysed asymmetric hydrogenation as a valuable synthetic tool for the preparation of chiral drugs. *Chem. Soc. Rev.* **42**, 728–754 (2013).
- Powell, M. T., Hou, D.-R., Perry, M. C., Cui, X. & Burgess, K. Chiral imidazolidine ligands for asymmetric hydrogenation of aryl alkenes. *J. Am. Chem. Soc.* **123**, 8878–8879 (2001).
- Wang, A., Wstenberg, B. & Pfaltz, A. Enantio- and diastereoselective hydrogenation of farnesol and O-protected derivatives: stereocontrol by changing the C=C bond configuration. *Angew. Chem. Int. Ed.* **47**, 2298–2300 (2008).
- Peters, B. K. et al. An enantioselective approach to the preparation of chiral sulfones by Ir-catalyzed asymmetric hydrogenation. *J. Am. Chem. Soc.* **136**, 16557–16562 (2014).

- Liu, G., Han, Z., Dong, X.-Q. & Zhang, X. Rh-catalyzed asymmetric hydrogenation of  $\beta$ -substituted- $\beta$ -thio- $\alpha,\beta$ -unsaturated esters: expeditious access to chiral organic sulfides. *Org. Lett.* **20**, 5636–5639 (2018).
- Yan, Q. et al. Highly efficient enantioselective synthesis of chiral sulfones by Rh-catalyzed asymmetric hydrogenation. *J. Am. Chem. Soc.* **141**, 1749–1756 (2019).
- Takaya, H. et al. Enantioselective hydrogenation of allylic and homoallylic alcohols. *J. Am. Chem. Soc.* **109**, 1596–1597 (1987).
- Maryanoff, B. E. & Reitz, A. B. The Wittig olefination reaction and modifications involving phosphoryl-stabilized carbanions. stereochemistry, mechanism, and selected synthetic aspects. *Chem. Rev.* **89**, 863–927 (1989).
- Thiemann, T. Wittig- and Horner–Wadsworth–Emmons olefination in aqueous media with and without phase transfer catalysis. *Mini-Rev. Org. Chem.* **15**, 412–432 (2018).
- Kita, Y. et al. Chloride-bridged dinuclear rhodium (III) complexes bearing chiral diphosphine ligands: catalyst precursors for asymmetric hydrogenation of simple olefins. *Angew. Chem. Int. Ed.* **55**, 8299–8303 (2016).
- Barton, D. H. R. & McCombie, S. W. A new method for the deoxygenation of secondary alcohols. *J. Chem. Soc.* **1**, 1574–1585 (1975).
- Nozaki, K., Oshima, K. & Utimoto, K. Facile reduction of dithiocarbonates with *n*-Bu<sub>3</sub>SnH-Et<sub>3</sub>B. Easy access to hydrocarbons from secondary alcohols. *Tetrahedron Lett.* **29**, 6125–6126 (1988).
- Lopez, R. M., Hays, D. S. & Fu, G. C. Bu<sub>3</sub>SnH catalyzed Barton–McCombie deoxygenation of alcohols. *J. Am. Chem. Soc.* **119**, 6949–6950 (1997).
- Drosos, N. & Morandi, B. Boron-catalyzed regioselective deoxygenation of terminal 1,2-diols to 2-alkanols enabled by the strategic formation of a cyclic siloxane intermediate. *Angew. Chem. Int. Ed.* **54**, 8814–8818 (2015).
- Foskey, T. J. A., Heinekey, D. M. & Goldberg, K. I. Partial deoxygenation of 1,2-propanediol catalyzed by iridium pincer complexes. *ACS Catal.* **2**, 1285–1289 (2012).
- Lao, D. B., Owens, A. C. E., Heinekey, D. M. & Goldberg, K. I. Partial deoxygenation of glycerol catalyzed by iridium pincer complexes. *ACS Catal.* **3**, 2391–2396 (2013).
- Schlaf, M., Ghosh, P., Fagan, P. J., Hauptman, E. & Bullock, R. M. Metal-catalyzed selective deoxygenation of diols to alcohols. *Angew. Chem. Int. Ed.* **40**, 3887–3890 (2001).
- Schlaf, M., Ghosh, P., Fagan, P. J., Hauptman, E. & Bullock, R. M. Catalytic deoxygenation of 1,2-propanediol to give *n*-propanol. *Adv. Synth. Catal.* **351**, 789–800 (2009).
- Dai, X.-J. & Li, C.-J. En route to a practical primary alcohol deoxygenation. *J. Am. Chem. Soc.* **138**, 5433–5440 (2016).
- Huang, J.-L., Dai, X.-J. & Li, C.-J. Iridium-catalyzed direct dehydroxylation of alcohols. *Eur. J. Org. Chem.* **2013**, 6496–6500 (2013).
- Bauer, J. O., Chakraborty, S. & Milstein, D. Manganese-catalyzed direct deoxygenation of primary alcohols. *ACS Catal.* **7**, 4462–4466 (2017).
- Yang, S., Tang, W., Yang, Z. & Xu, J. Iridium-catalyzed highly efficient and site-selective deoxygenation of alcohols. *ACS Catal.* **8**, 9320–9326 (2018).
- Isomura, M., Petrone, D. A. & Carreira, E. M. Coordination-induced stereocontrol over carbocations: asymmetric reductive deoxygenation of racemic tertiary alcohols. *J. Am. Chem. Soc.* **141**, 4738–4748 (2019).
- Liu, J., Krajangsri, S., Yang, J., Li, J.-Q. & Andersson, P. G. Iridium-catalysed asymmetric hydrogenation of allylic alcohols via dynamic kinetic resolution. *Nat. Catal.* **1**, 438–443 (2018).
- Krajangsri, S. et al. Tandem Peterson olefination and chemoselective asymmetric hydrogenation of  $\beta$ -hydroxy silanes. *Chem. Sci.* **10**, 3649–3653 (2019).
- Kerdphon, S. et al. Diastereo- and enantioselective synthesis of structurally diverse succinate, butyrolactone, and trifluoromethyl derivatives by iridium-catalyzed hydrogenation of tetrasubstituted olefins. *ACS Catal.* **9**, 6169–6176 (2019).
- Poremba, K. E., Kadunce, N. T., Suzuki, N., Cherney, A. H. & Reisman, S. E. Nickel-catalyzed asymmetric reductive cross-coupling to access 1,1-diaryllkanes. *J. Am. Chem. Soc.* **139**, 5684–5687 (2017).
- Berardi, F. et al. 4-(Tetralin-1-yl)- and 4-(naphthalen-1-yl)alkyl derivatives of 1-cyclohexylpiperazine as  $\sigma$  receptor ligands with agonist  $\sigma_2$  activity. *J. Med. Chem.* **47**, 2308–2317 (2004).
- Church, T. L., Rasmussen, T. & Andersson, P. G. Enantioselectivity in the iridium catalyzed hydrogenation of unfunctionalized olefins. *Organometallics* **29**, 6769–6781 (2010).

## Acknowledgements

The Swedish Research Council (VR), Stiftelsen Olle Engkvist Byggmästare, the Carl Tryggers Stiftelse, Knut and Alice Wallenberg foundation (KAW 2016.0072 and KAW 2018.0066) supported this work. J.J. thanks the Scientist Development Project Commemorating His Majesty the King's 84<sup>th</sup> Birthday Anniversary, Chulabhorn Graduate Institute. We are also thankful to D.A. Tanner and M. Nolan for proofreading the manuscript.

**Author contributions**

P.G.A. conceived and designed the experiments. J.Z., J.J., B.B.C.P., J.G. and S.P. performed experiments and prepared the Supplementary Information. M.S.G.A. performed the computational studies. P.G.A. and J.Z. wrote the paper. All authors discussed the results and commented on the manuscript.

**Competing interests**

The authors declare no competing interests.

**Additional information**

**Supplementary information** is available for this paper at <https://doi.org/10.1038/s41929-019-0375-7>.

**Correspondence and requests for materials** should be addressed to P.G.A.

**Reprints and permissions information** is available at [www.nature.com/reprints](http://www.nature.com/reprints).

**Publisher's note** Springer Nature remains neutral with regard to jurisdictional claims in published maps and institutional affiliations.

© The Author(s), under exclusive licence to Springer Nature Limited 2019